Novel concept of renewables association with synchronous generation for enhancing the provision of ancillary services

A. Attya[1*], O. Anaya-Lara[2] and W. E. Leithead[2]

1: Department of Engineering & Technology, University of Huddersfield, Huddersfield, UK

2: Wind Energy & Control Centre, University of Strathclyde, Glasgow, UK

*Corresponding author: a.attya@hud.ac.uk

Abstract: Renewable energy sources are foreseen as a provider of full range of ancillary services. An innovative concept of alignment between renewable power generation elements and synchronous generators is proposed: Renewables Association with Synchronous generators (RAS). It mitigates the dependence on direct frequency measurements, which are prone to noise and lack of accuracy, and enables perfect coordination between the responses of renewable and conventional power plants. RAS relies on a leader synchronous generator, connected at the point of common coupling of the renewable power plant or close to it. This synchronous generator is able to provide ancillary services (e.g. frequency support and reactive compensation). The renewable power plant is controlled to provide such services similar to the leader synchronous generator, but scaled down/up to match the rating of the renewable power plant by integrating supplementary controllers that are associated with the synchronous generator response. Two approaches are proposed to provide voltage support, besides a supplementary frequency support controller. These RAS-based voltage and frequency support methods are compared to other methods proposed in the literature. Results show the positive impact of RAS concept on the provision of active power and reactive compensation to tackle frequency and voltage events respectively, following the response of the leader synchronous generator. DIgSILENT PowerFactory is the applied simulation environment.

Nomenclature

AS	Ancillary services
D_F	De-loading factor
f_{low}	Frequency deadband in conventional support method
f^m_d	Frequency deviation to release full support
HVDC	High voltage direct current link
k_1, k_2	Coefficients of RAS-based frequency support method
PCC	Point of common coupling
PEC	Power electronic converters
PMU	Phasor measurement unit
P^o_{ref}	Wind turbine optimal active power reference
P_{ref}	Wind turbine actual reference active power
P_{SG}, Q_{SG}	Active and reactive power at the leader generator bus respectively
pu	Per unit
Q^o_{ref}	Default reference reactive power

Q_{ref}	Actual reference reactive power
RAS	Renewables association with synchronous generators
REC	Receiving end converter
RES	Renewable energy sources
$RoCoF_m$	Maximum rate of change or frequency
SG	Synchronous generator
V_{PCC}	Voltage at PCC (suffix *o* stands for nominal value)
V_{RAS}	Voltage limit to initiate RAS voltage support
v_{SG}	Voltage at leader generator bus
WTG	Wind turbine generator

1. Introduction

The foreseen high penetration of Renewable energy sources (RES), mainly wind energy into power systems imposes strong challenges regarding the provision of ancillary services (AS) [1, 2]. The key challenge of RES, except hydro, is their connection method to the grid as they are decoupled through power electronics converters (PEC), which act as an interface between the energy harvesting systems (e.g. solar panels, wind turbine generators; WTGs), and the AC grid [3]. Hence, the PEC screen the variations and events on the grid side, and handle it rapidly without being observed by the WTGs. Consequently, the WTGs do not naturally provide conventional frequency and voltage support similar to synchronous generators (SGs). Conversely, a conventional SG is directly connected to the AC grid, which enables it to respond to all changes in voltage and frequency in the grid using its exciter and governor systems. The main differences between the two generation technologies are summarized in Table 1.

Table 1. Differences between SGs and RES in provision of AS (PCC: point of common coupling)

Point of comparison	Conventional generation	Renewable generation
Energy source	Dispatchable fossil fuel	Predictable and intermittent
Connection to AC grid	Direct connection	Decoupled by power electronics
Grid frequency sensing	Direct through generator speed	Measured at a certain point of the grid
Response to frequency events	Inertia (natural), primary and secondary	Integrative inertia and primary response using special controls
Grid voltage sensing	Direct at connection point	Measured at PCC
Response to voltage events	Reactive compensation using exciter	Low voltage ride-through using special controls in WTG and/or receiving converter station

Frequency response is executed by synchronous power plants through a natural response, i.e. rotating parts inertia, and primary response provided by the governor, i.e. droop setting [4]. Frequency measurement is not required to drive both types of response, where the governor receives the deviation in generator speed compared to its synchronous speed, which is the nominal frequency of the grid, and regulates the input mechanical power (e.g. valve opening in case of steam turbines) to maintain the nominal speed. The literature proposed a wide range of control methods to enable WTGs to provide frequency support, namely synthetic inertia and primary response [5, 6]. The provision of frequency support by wind power, includes three technical obstacles, intermittent

wind speed that makes the provided supportive active power highly uncertain, the applied method to secure active power reserve during normal operation, and frequency measurements. There are two main concepts to secure power reserve by wind power, kinetic energy (KE) extraction and droop de-loading. The KE extraction method does not deviate the WTG from the traditional Maximum Power Tracking (MPT) operation, where during frequency drops the rotor speed decelerates, and the extractable KE is converted into electrical energy to deliver power support retaining the balance between generation and demand [7, 8]. The de-loading concept relies on continuous de-rating of the WTG output to secure a certain margin between the available optimum output and the actual de-loaded output. This margin can be a constant value or a ratio of the available production, these two approaches are known as Balance and Delta de-loading respectively [9]. With the previous methods rely on frequency measurements, where the frequency deviation is the main input to the integrated supplementary controllers, and it is communicated to WTG or wind farm (WF) controls to determine the required power support. The provided support does not follow a certain predetermined pattern, but it depends on the incident wind speed, applied support method and event severity. There is also a more generic concept of Virtual Synchronous Machine (VSM) where the power electr0nics coupled system is controlled to provide responses acting as a virtual SG. This concept has been applied to WFs [10] and electric vehicles as well to provide frequency support [11]. There is also a strong research and industry trend to curtail this challenge by enabling the demand side response, including electric vehicles, where certain uncritical loads can be curtailed to mitigate frequency drops and provide artificial and passive frequency support on behalf of RES [12, 13].

The WTGs/WFs are required to ride through system faults and provide reactive compensation contributing to voltage recovery during and shortly after voltage events [14, 15], where this type of AS is always prioritized over frequency support [16]. This splits into two tasks, the WTGs/WF must keep connected to the grid and does not trip, within the early stage of the fault without causing any damage to the WTG [17]. Afterwards, it has to inject reactive power/current to mitigate the voltage drop and recover the nominal voltage. This process is executed in SG by the field winding exciter, which increases the field current when the voltage across the machine terminals drops [4]. However, supplementary controllers are integrated to regulate the d and q components of the current (i_d and i_q) to inject a certain level of reactive current by WTG grid-side converter or the onshore converter stations that deliver WF power, without violating their ratings and controllers' limitations [18-20].

In the context of the previous discussion, this paper presents the novel RES association with synchronous generators concept (RAS) to enhance the provision of frequency support and reactive compensation by wind energy. The offshore WF, integrated into the investigated test system, is connected to an AC grid through a high voltage direct current link (HVDC). A supplementary controller is proposed and integrated into the generic double-fed induction generator (DFIG) WTG model to associate the provided frequency support by each WTG in the WF with a leader SG located near PCC of the onshore converter station. Two control approaches are proposed and integrated into the Receiving End Converter (REC) controller to mimic the response of the leader SG during voltage dips. Thus, the application of RAS is examined on two fronts, WTGs and the onshore converter station. The proposed controllers are compact and avoid complicated methods as they rely on one or two inputs received from simple measurements at the leader SG bus. These

measurements are utilised to manipulate the set-points of active power and reactive power of WTG and REC controllers during frequency and voltage events respectively. The application of this concept is expected to avoid the dependence on frequency measurements and make the provision of AS more predictable, as it follows the conventional patterns of SGs responses during critical events. Both voltage and frequency controls are integrated and operational simultaneously, which is an additional aspect of novelty because most of the research studies, oriented to the provision of ancillary services, focused on one AS only ignoring the possible mutual interactions if more than one support method is integrated. Moreover, the proposed concept is valid for AC and DC connected wind power assets, either as single units and/or the whole WF represented by the interconnecting converter station. The performance of the proposed controls and the system responses are compared to the corresponding ones when no support is provided or when conventional support methods are applied to ensure the comprehensiveness of the implemented study. This concept can be applied using the available SGs in the network, hence there is no need to build special SGs. This will help Transmission System Operators to perform more accurate and confident planning and operation studies of power systems under high penetration of wind energy or any type of RES because this concept can be applied to PEC-based power plants including solar and tidal energy.

2. RAS concept

The mismatch between WTG/WF responses and the simultaneous reactions of the conventional SGs to system events raises further stability issues in power systems, especially when WFs replace conventional power plants, i.e. shutdown thermal power plants. It is essential to develop control methods that enable WTGs and WFs to mimic or follow the conventional reactions of SGs during critical system events. The concept of RAS relies on slaving RES elements (e.g. wind turbines, holistic controls of WFs, etc.) to a leader SG during critical events including frequency excursions and voltage dips. Accordingly, the WTGs and/or the WF are temporarily associated with the pre-determined physical conventional SG not a virtual generator, or a PEC-based generation system (e.g. a battery storage system which is the case in [21]). The proposed concept can reduce the uncertainties in the provided support during critical frequency and voltage events, such that each renewable power plant follows the response of a nearby SG instead of adopting its own method to provide frequency and voltage support. Therefore, the provided support can pertain the conventional profiles of a SG. However, the uncertainty related to the amount of support, according to the intermittent nature of RES generation, i.e. wind speed conditions, is still present. In addition, the proposed method avoids the need to use frequency measurements, which is essential to other support methods by wind energy, however such measurements rely on accurate settings of the Phase-Locked Loop (PLL) [22], and prone to frequency oscillations. The proposed concept relies on the measurement of voltage and the estimation of active and reactive power at the SG bus (v_{SG}, P_{SG} and Q_{SG} respectively) using a Phasor measurement unit (PMU) as illustrated in Figure 1. The measured signals are converted to per unit values (pu) to avoid the mismatch between the ratings of the leader SG and the associated WTG/WF, hence it is required to follow the pattern of the SG response not the actual magnitude of its active and reactive power generation.

The RAS concept is valid for AC and DC connected WTGs and/or the whole WFs, as it can be adopted through supplementary controllers that enable WTG/WF to mimic a SG that is physically present in

the system. The concept can be applied to the power electronics controls of the HVDC converter station transmitting the WF power to the grid at the PCC. RAS concept does not require the installation of additional equipment, i.e. there is no need to install a special synchronous generator to act as leader SG as this can be an uneconomic solution. The system operator has just to select a SG to which the WF is associated, taking into consideration the rated power equivalency and distance to PCC. The location of the leader SG does not form a key barrier, ideally it should be connected at the PCC of the WF to ensure that the SG responds to the same event seen by the WF or the converter station connecting it. RAS enables high matching between the response of RES and SGs, which mitigates the uncertainties involved in the response of RES to voltage and frequency events. This facilitates the understanding and prediction of power system dynamics under high penetration of RES, as they are able to mimic the physically connected SGs. The merits of such concept are enumerated in Figure 1, where precise and timely event detection, and perfect coordination between generation assets are among the key advantages.
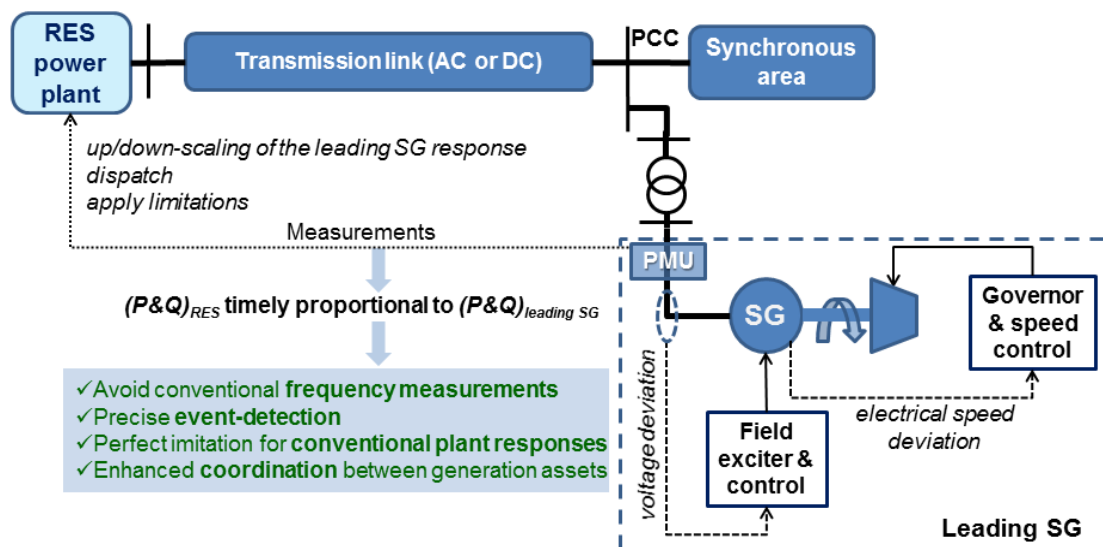

Figure 1. Conceptual representation of RAS concept.

In this paper, RAS concept is applied to enhance the provision of frequency support by each WTG, meanwhile reactive compensation is provided by the onshore converter of an HVDC link connecting an offshore WF to the grid, where the HVDC station provides voltage support on behalf of the WF. In the offered frequency and voltage support controls, basic measurements at the leader SG are innovatively utilized to drive the active and reactive power generation of the wind power assets during and shortly after the critical voltage and frequency events. In addition, the proposed methods do not incorporate many parameters that require challenging tuning procedures or online amendments, which offers a reasonable complexity level without constraining the operability of the proposed methods. This also saves the computational time, which ensures that the provided AS is timely following the leader SG and grid dynamics.

The aspect of selecting the leader SG will require further investigations, where the SG location in the grid, rating, type and main control will be the key factors. As an illustration, the leader SG location should not be so far from the PCC as it will experience a different voltage level with a

relatively high margin compared to the WF. The proposed voltage support method considers the difference between the voltage levels at the lead SG and the associated WF as explained later in Section 4. In addition, the WF is typically required to respond to voltage events at or close to the PCC when the voltage falls below a certain threshold. It is also essential to design supplementary controllers that can directly fit in the conventional controls of WTGs and amend the control signals and set-points already available in conventional controls of WTGs and converter stations, which is considered in this paper. The size of the leader SG is preferred to be comparable to the size of the associated WF, which can have an improved impact on the system such that the response of the SG is not highly up or down-scaled compared to the WF rating. The type of generation of the leader SG can be decided based on the main required AS, for example, if the WF is required to be responsive to frequency drops, a leader SG can be selected as a gas power plant, while if it is required to act as a balancing power provider a hydropower plant can be a better choice. The applied governor and exciter controls of the leader SG play a role as the WTG/WF copies the response of the leader SG that is mainly shaped by these two controllers.

3. Frequency support

The provision of frequency support is a challenging issue for PEC interconnected generation assets, including wind energy. The common practice is to sacrifice a proportion of its output power at all times to secure a certain amount of power reserve. The regulation of this reserve during frequency drops is an additional challenge, where the proposed methods in the literature focus on driving WTGs/WFs in a similar way to SGs [7, 23]. In this paper, frequency support is provided by a RAS-based method and compared to a conventional de-loading method. Both support methods amend the optimal reference active power signal fed into the comprehensive controller model implemented in the WTG model offered by DIgSILENT library.

3.1.   Conventional frequency support method

The applied method can be classified as Delta de-loading, where the WTG output is de-loaded continuously by a constant ratio (D_F). The *available* optimal output (P^o_{ref}) is the WTG output when it follows the conventional operation technique Maximum Power Tracking (MPT). The active power set-point is reduced by D_F, meanwhile the rotor speed is regulated around its nominal value according to the incident wind speed during normal frequency conditions, i.e. normal operation mode. The ratio P^o_{ref}/P_{ref} is manipulated using (1),

$$\frac{P_{ref}}{P^o_{ref}} = - \begin{cases} D_F, & f \geq f_{low} \\ D_F \times \left(\frac{f_o - f}{f_d^m} - 1 \right), & (f_o - f_d^m) < f < f_{low} \\ 0, & f \leq (f_o - f_d^m) \end{cases} \tag{1}$$

where f_o is the nominal system frequency, and P_{ref} is the actual reference active power. The applied value of D_F is 20%, which is a relatively high de-loading ratio to emphasis the impact of the proposed methods and illustrate the occurring dynamics during the support process. When the frequency violates a safe deadband (f_{low}), the de-loading ratio is curtailed regularly by a droop gain until the

frequency reaches a predefined threshold (f^m_d), where the WTG produces its available output as illustrated in the control block diagram in Figure 2(a). This procedure smoothens the system response. The pitch de-loading is deactivated when the incident wind speed approaches the rated wind speed of the WTG to curtail the lost energy due to de-loading. It is of note that, pitching is activated by default at high wind speeds to maintain the WTG output and rotor speed within safe limits, however, at frequency events, pitch angle can be exceptionally reduced to allow a slight overload of the WTG for a short predefined duration, which relies on the specifications of the WTG to avoid excessive heating or any sort of damage as indicated by the manufacturer instructions [6].
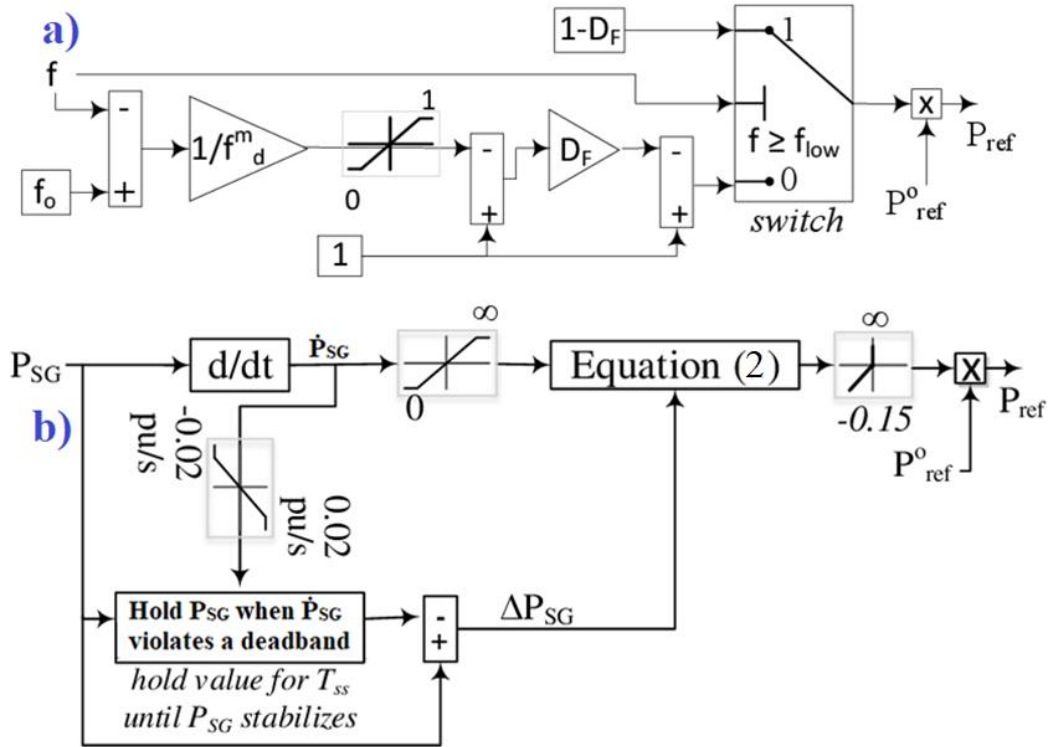

Figure 2. Integrated supplementary frequency support controllers: a) conventional, b) RAS-based.

3.2 RAS-based method

A novel supplementary controller is proposed to '*copy*' the response of a leader SG during frequency events without the need to measure and use network frequency in the WTG controls. This controller applies Delta de-loading, as the WTG output is de-loaded by D_F during normal operation. The same value of D_F is used to allow a fair comparison with the conventional support method explained in the previous section. When the power system suffers a frequency drop, de-loading ratio is regulated to increase the WTG output following the response of the active power generated by the leader SG to retrieve the balance between generation and demand in the power system. The proposed controller tunes P_{ref} of the WTG as a ratio of the available power (P^o_{ref}) using (2) and (3), the controller schematic is illustrated in Figure 2(b),

$$\frac{P_{ref}}{P^o_{ref}} = 1 - D_F + D_F \times (k_1 \times \frac{\dot{P}_{SG}}{\dot{P}^m_{SG}} + k_2 \times \frac{\Delta P_{SG}}{\Delta P_R})$$

(2)

$$k_1 + k_2 = 1 \ where \ k_1 \geq 0 \ and \ k_2 \geq 0$$

$$\dot{P}_{SG}^m = \frac{RoCoF_m}{R_{SG} \times f_o} \text{ and } \Delta P_R = \frac{f_m^d}{R_{SG} \times f_o} \quad (3)$$

where the rate of change of SG power ($\dot{P}_{SG}$) is compared to a predefined maximum value ($\dot{P}_{SG}^m$), which relies on the worst allowed rate of decay of frequency (RoCoF$_m$) decided by the grid codes, and beyond this limit, the RoCoF protection relays may trip, ΔP_{SG} is the power step provided by the SG, ΔP_R is the droop base value of ΔP_{SG}. R_{SG} is the frequency droop of the leader SG in per unit, f_o is the nominal frequency, k_1 and k_2 are dimensionless gains acting as weighting factors of inertia and droop support. It is of note that, $\dot{P}_{SG}^m$ can be also related to the time inertia of the leader SG in seconds instead of R_{SG}, however, this is not preferable, because the time inertia is an estimated and natural parameter of the SG while R_{SG} is a tuneable control parameter in the SG governor.

The proposed method tunes P$_{ref}$/P$^o_{ref}$ based on two components, first is related to the instantaneous power support provided by the SG, and the second relies on the rate of change of P$_{SG}$. Both components are normalized with respect to two constant parameters, i.e. k_1 and k_2, which can be tuned to comply with the grid code, and operational constraints, namely $\dot{P}_{SG}^m$ and R$_{SG}$.

The applied time delay (T$_{ss}$) is to ensure that de-loading is recovered to D$_F$ after the leader SG is re-dispatched to a new generation level without excavating the frequency event or triggering a new one. ΔP_{SG} is kept constant to its latest value just before $\dot{P}_{SG}$ tending to zero until T$_{ss}$ is finished. The instantaneous recovery to full de-loading after T$_{ss}$ can trigger further frequency drops, hence, the de-loading rate is limited as shown in Figure 2(a). The numerical values of the applied parameters of this control method are found in Table 2, and a simplified illustration of the two methods is shown in Figure 3. The privilege of avoiding frequency measurements is clear where the active power generated at the SG bus is communicated to the RAS control. P$_{SG}$ can be estimated using the voltage and current measurements from a PMU at the desired location or other tools including power meters of high sampling resolution (e.g. 2 readings/s).
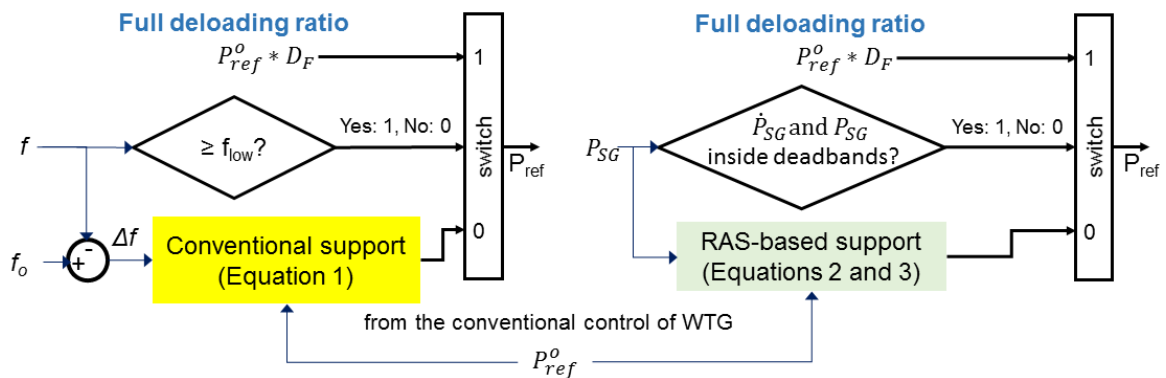

Figure 3. Conceptual schematic of the integration of the two support methods

Table 2. Values of RAS frequency support parameters

D$_F$	0.2 pu (max. de-loading rate 0.15 pu/s)	R$_{SG}$	0.04 pu
f$_o$, f$_{low}$	50 Hz, 49.95 Hz	f^m_d	0.3 Hz
RoCoF$_m$	±0.3 Hz/s	T$_{ss}$	30s
k$_1$	0.3	k$_2$	0.7

This paper focuses on frequency drops, as it is required to provide more active power, which can be challenging to wind power. Meanwhile, over-frequency events can be treated by other generation assets by reducing their outputs, while the wind power is permanently de-loaded by the predetermined D_F ratio to maintain the availability of power reserve. In addition, the proposed method can be applied in the opposite way when the rate of change of P_{SG} is negative, which indicates an over-frequency event, i.e. curtailing the wind generation following the leader SG. It is worth mentioning that, the frequency support provided by WTG/WF relies on the technology and controls of the leader SG. As an illustration, a faster response is expected if the WTG/WF is associated with a gas power plant, while the response is slower in case of hydropower plants. The response also depends on the SG governor droop value and inertia. The responsive nature of the PEC interconnecting the WTG/WF allows it to follow the SG quickly enough compensating potential communication latency.

It is of note that, this paper is dedicated to proposing and implementing the RAS concept rather than its application to dispatch the frequency support from each WTG within a WF. Further research will propose a holistic WF controller to apply RAS concept, and allocate the required frequency support to each WTG. In addition, the applied test system treats groups of individual WTGs as an aggregate WTG with an equivalent rated power as explained in Section 5, hence, the implemented RAS support method is exploited from a WF point of view.

4. Voltage support

Applying the same analysis approach in frequency support, voltage support is provided through two methods, a conventional one or using a RAS-based method.

4.1 Conventional voltage support

The Receiving end converter of the interconnecting HVDC station can ride through faults relying on conventional methods, which supervise the reference value of the i_q current component within the limits of the PQ capability curve of the converter [24]. However, the developing dynamics depend on the gains of the proportional-integral controller that derives the set-points of the AC voltage and the reactive power, in addition to the voltage threshold at which the fault mode is enabled. These parameters require careful tuning to ensure the compliance with the applied grid code without compromising the safety of the converter station. The three control methods of a REC in HVDC links are: voltage control, droop control and reactive power control. The applied conventional control applies the common voltage control mode, where the reactive injection is managed through a proportional-integral to maintain the voltage level at the REC within acceptable margin, the generic parameters of this method as applied in DIgSILENT library are found in the appendix.

4.2 RAS-based method

A supplementary control method is proposed such that the reference reactive compensation of the REC is copying the response of a SG, which is relatively close to PCC. The voltage at the SG bus and reactive power of the leader SG is estimated and communicated at the bus interconnecting the SG

to the network. This signal is received in per unit to accommodate the different ratings of the leader SG and the associated REC, and it is used to manipulate the reference reactive power (Q_{ref}) of the REC controls such that it mimics the response of the leader SG. The support mode is activated when the observed voltage at PCC (V_{PCC}) falls below a certain limit (V_{RAS}). The parameter V_{RAS} decides when the default reactive power set-point (Q^o_{ref}), indicated by the REC conventional controller, is replaced by the incoming set-point from the RAS supplementary controller (Q_{ref}) during voltage dips. Two approaches are proposed to obtain Q_{ref}, first is to use the estimated reactive power generation of the leader SG (Q_{SG}) to be followed by REC. The second approach considers the divergence between V_{PCC} and v_{SG}, hence Q_{SG} is obtained by dividing Q_{RAS} by v_{SG} to obtain an approximate value of the SG reactive current then multiply it by the nominal value of V_{PCC} (V^o_{PCC}), which is assumed to be 1 pu, as illustrated in Figure 4. Q_{SG} should be larger than Q^o_{ref} in both approaches since it is beneficial to inject a higher amount of reactive power/current during voltage dips. It is a common practice to set Q^o_{ref} to zero as REC is preferred to operate at unity power factor under normal conditions similar to the grid side converter of WTG. The applied converter control is DC voltage/reactive power regulation [24], the detailed explanation of such conventional control method is out of scope of this paper. The reactive power set-point is fed to the proportional integral i_d and i_q controller to adjust their values to comply with the requirements. The details and the explanation of the main controller are not included as they are vastly discussed in the literature [25]. The tuning of V_{RAS} relies on the location of the SG i.e. the impedance between the SG bus and the PCC, and the PQ capability of the REC. V_{RAS} is assumed to be 0.85 pu inspired by a fault ride through patterns in some grid codes [14]. This value is related to the voltage limit at which reactive compensation should be activated according to grid code requirements. Proposing a deterministic method to evaluate V_{RAS} is an objective of future work.

The proposed supplementary controller can be integrated into the generic main controls of a WTG as shown in Figure 10 in the Appendix, which is an illustrative schematic to provide deeper details on the actual integration of the proposed controller to the sophisticated and comprehensive model of the onshore HVDC station in DIgSILENT.
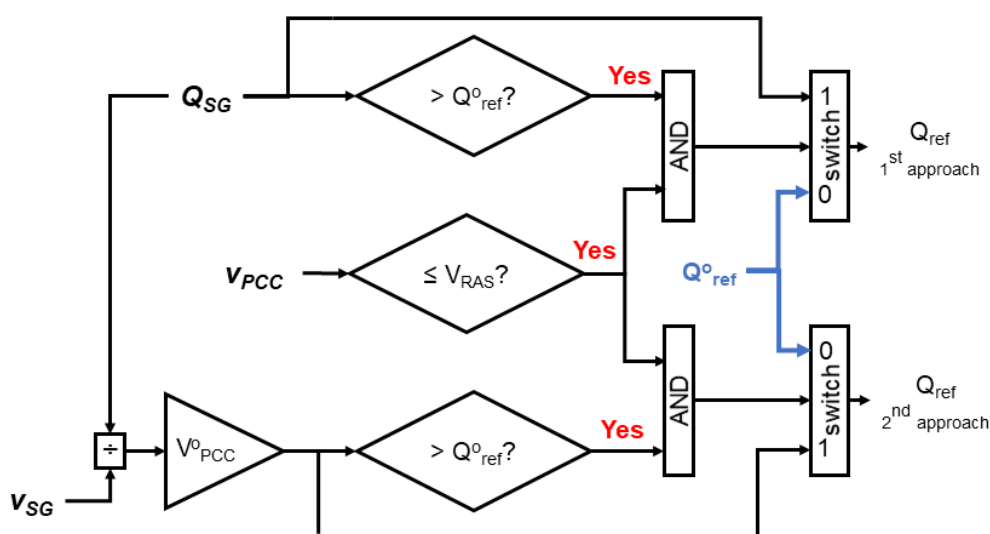

Figure 4. RAS voltage support supplementary control.

Generally, a constant communication time delay applies to all the support methods examined in this paper. In conventional methods, there is a delay to communicate the frequency/voltage at the desired measurement point. Likewise, in RAS-based methods, the communication latency applies to the received measurements from the PMU at the bus of the leader SG. The modern PMUs, which are synchronised with GPS and time stamps of very high resolution, provide high accuracy and short latency of 10-30ms [26], hence communication latency is simulated by applying an average time delay of 15ms, where the shape of the measured signal is preserved without corruptions [27]. Actually, the timescale of communications delays should not affect the provision of frequency support because any interconnected generator is expected to start reacting to a frequency event within 0.5s, which is much longer than the average time delay caused by communicating the necessary control signals.

5. Test system

The test system is carefully designed to cover all the concerns related to the provision of AS by RES. The system is composed of an offshore WF: 400 MW installed capacity (80x5 MW DFIG), which is connected to an external grid via a bi-pole HVDC link of 100 km length, 150 kV rated voltage and 450 MW capacity. A 510 MVA synchronous power plant is connected to the grid via an AC over-head transmission line of 30 km as shown in Figure 5(a). The HVDC link voltage and delivered power are regulated by Voltage Source Controller 6-pulse converter stations [28]. The proposed concept is valid for any power electronics interfaced generation, hence, it is applicable to DFIGs and Full rated converter WTGs (Type 4), however, the implemented test system includes a DFIG-based WF as this type is still dominating the integrated wind energy systems worldwide. The WF generation is collected through five feeders, each feeder is connecting a ring of WTGs. The three feeders each connects a ring of 20 WTGs, while the fourth and fifth each connects a ring of 10 WTGs. The WTGs connected through the same ring, i.e. same main feeder, are modelled as an aggregate WTG of an equivalent installed capacity (e.g. first ring with 20x5 MW installed capacity). However, the WTGs connected to the fifth ring are modelled as 10 single units. The detailed representation is reflective, as the proposed concept and the corresponding frequency support methods are applied to each individual WTG, hence this model will allow further investigations in the future. The WF layout is shown in Figure 5(b). The WTG model is the DIgSILENT 5 MW-DFIG detailed template including the turbine, shaft, PQ controls of converters, and protection devices, where the default values of the parameters are applied [29]. The grid model has 10 GVA short circuit capacity and 8s acceleration time, and is modelled as a PV bus of primary and secondary response coefficients of 350 and 650 MW/Hz resp. The short circuit ratio of the grid compared to WF capacity is 25, reflects an average strength grid, moderately resistible to transients [30]. The RAS concept is applicable in large power systems, where the size and level of complexity of the entire power system does not curtail its application. In particular, the proposed concept is focused on making RES follows the profile of a certain conventional power station during critical events, and hence a SG is not included in the aggregated grid model to act as the leader SG in the proposed method. It is beneficial to the power system stability to select the leader SG to be highly responsive, hence thermal power plants, i.e. steam and gas plants, are preferred on hydropower plants. The SG is modelled by the full detailed generator, steam turbine-governor and exciter generic models IEEE_G1 and IEEE_X1 respectively

[31, 32] that are embedded in DIgSILENT library. The values of the key parameters of the leader SG governor and exciter are tabulated in the appendix.
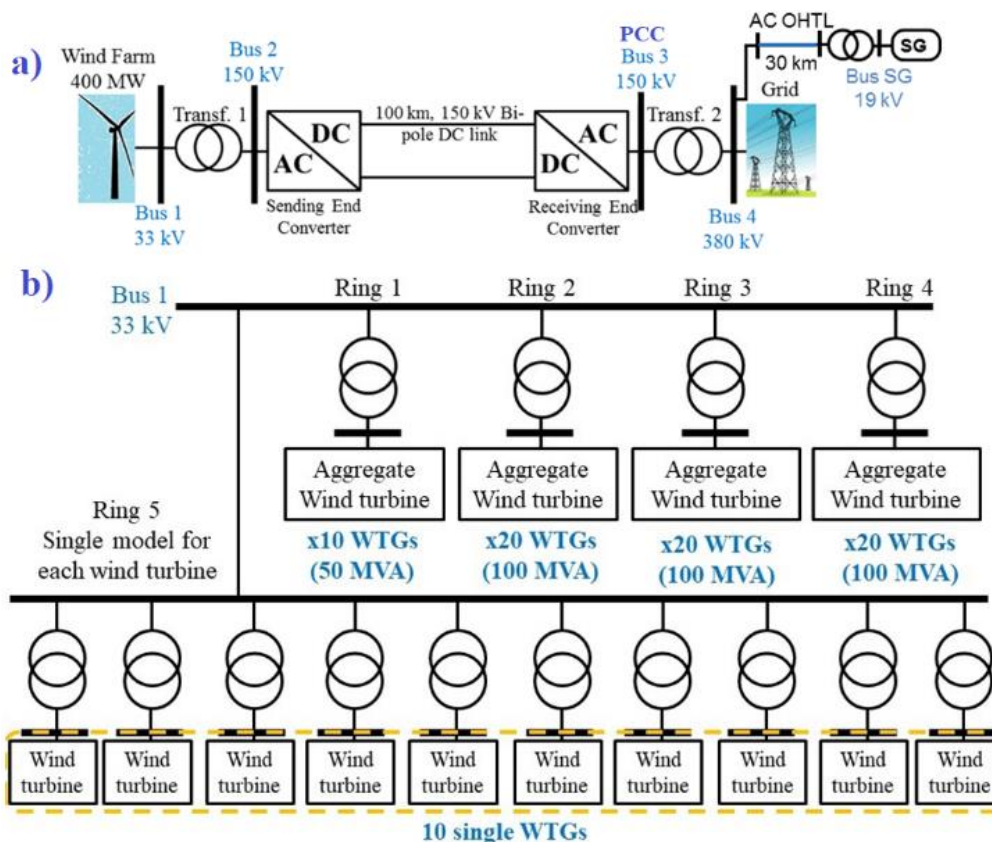

Figure 5. Test system a) Main network, b) WF layout.

6. Scenarios and results

The applied scenarios are described and the results obtained are discussed in this section. Both voltage and frequency support supplementary controllers are integrated into the test system, although the common practice in the literature is to test only voltage or frequency support methods independently not simultaneously. This approach is adopted to ensure the compatibility of both control methods, and that they are not conflicting with each other. It is preferred to prioritize voltage support such that frequency support is deactivated when the voltage is violating a certain deviation margin e.g. ±0.1 pu, this is also aligned with the requirements of many grid codes [16].

The discussion of results focuses on the foreseen positive impact of the proposed concept and corresponding supplementary controls on the test power system dynamics (i.e. voltage and frequency), and their capability to make the associated wind power assets copy the typical responses of the leader SG. The results have also revealed the internal dynamics of the integrated controls, and the alignment of their operation with the design targets.

6.1 Voltage support

The impact of the two RAS voltage support approaches when applied to REC controller separately is compared to a base case without any support, and a third case where conventional AC voltage

support is activated. In all cases, Q^o_{ref} is set to zero, which is the common practice to operate the WTG/WF/HVDC station at a unity power factor.

Scenario 1: 3-phase symmetrical very severe fault of impedance $0.07 + j0.07\ \Omega$ at Bus 3 (PCC).

Scenario 2: 3-phase symmetrical fault of impedance $1.4 + j1.4\ \Omega$ at the PCC to cause a less severe voltage dip compared to Scenario 1.

Both faults occur at t = 2s and continue for 200ms. The PCC is selected to apply the fault to exploit a worst case scenario, as it mitigates the capability of the WF to provide voltage support. Applying two events of different severity also reflects the impact of the lead SG proximity from the associated WF.

The focus is at the behaviour of reactive current injection that clearly improves in Scenarios 1 and 2 after the application of support methods as detailed in the following discussion. Results show a very severe voltage dip in Scenario 1 in Figure 6(a), which makes the REC unable to provide any reactive power during the fault, but reactive current can be injected according to the applied support control method as shown in Figure 6(b) and Figure 6(c). The REC absorbs reactive current, i.e., blue solid line in Figure 6(c), without the application of any support method, while it is enabled to supply reactive current during the fault with either of the two support methods. The deviations between the conventional and RAS-based methods are minor, where the RAS-based method rebounds slightly faster to its initial state after the fault is cleared. Although the incident voltage dip is very severe, it is judged to be acceptable or not according to the grid code in force. In particular, the applied fault is cleared after 200ms which is acceptable by most of the European grid codes [14], further research is also conducted on the evolution of grid codes under high penetration of wind energy in [16]. Therefore, this event can occur in real power systems, and it does not violate the common requirements of grid codes. The results also show that the voltage at the AC offshore bus is not affected by the onshore event due to the decoupling between the two AC systems by the HVDC link. At this severe scenario, the application of both support methods does not improve the voltage dip, as it occurs at the AC bus of the REC. It is of note that, the RAS controller is activated as long as the dip occurs, as the voltage level is lower than the predetermined threshold V_{RAS}. The delivered active power by the REC falls to almost zero during the dip because the voltage is very close to null, this triggers transients through the DC link as the power is still generated by the WF from the sending end station, and however, this is out of scope of this paper. Actually, such transients occur with or without the RAS controller that aims to enhance the reactive current compensation of the REC imitating the leader SG response. This target is achieved where the reactive current of REC during the fault is copying the same pattern of the SG as shown in Figure 6(b), however, it cannot provide the same magnitude as the fault location is closer to REC. The conventional method provided an aligned response. The two proposed approaches of Q_{ref} estimation achieved the almost same impact in Scenario 1 due to its severity, results are not shown due to space limitations.

The response of SG is displayed for one case only as the examined method does not have an impact on the dynamics of the SG. This also improves the visibility and clarity of the figures, which applies to Figures 6, 7 and 8. The key control signals are shown in Figure 6(e), where the 2nd Approach pushes Q_{ref} to the limit because dividing Q_{SG} by v_{SG} increases Q_{ref}, where v_{SG} is always less than 1 pu

during the fault. The 1st Approach typically follows the SG injecting reactive current to mitigate the dip at the AC bus of REC. The location of the SG plays role in RAS voltage support, where it has an impact on v_{SG}, i.e. v_{SG} drops to 0.63 pu in Scenario 1.
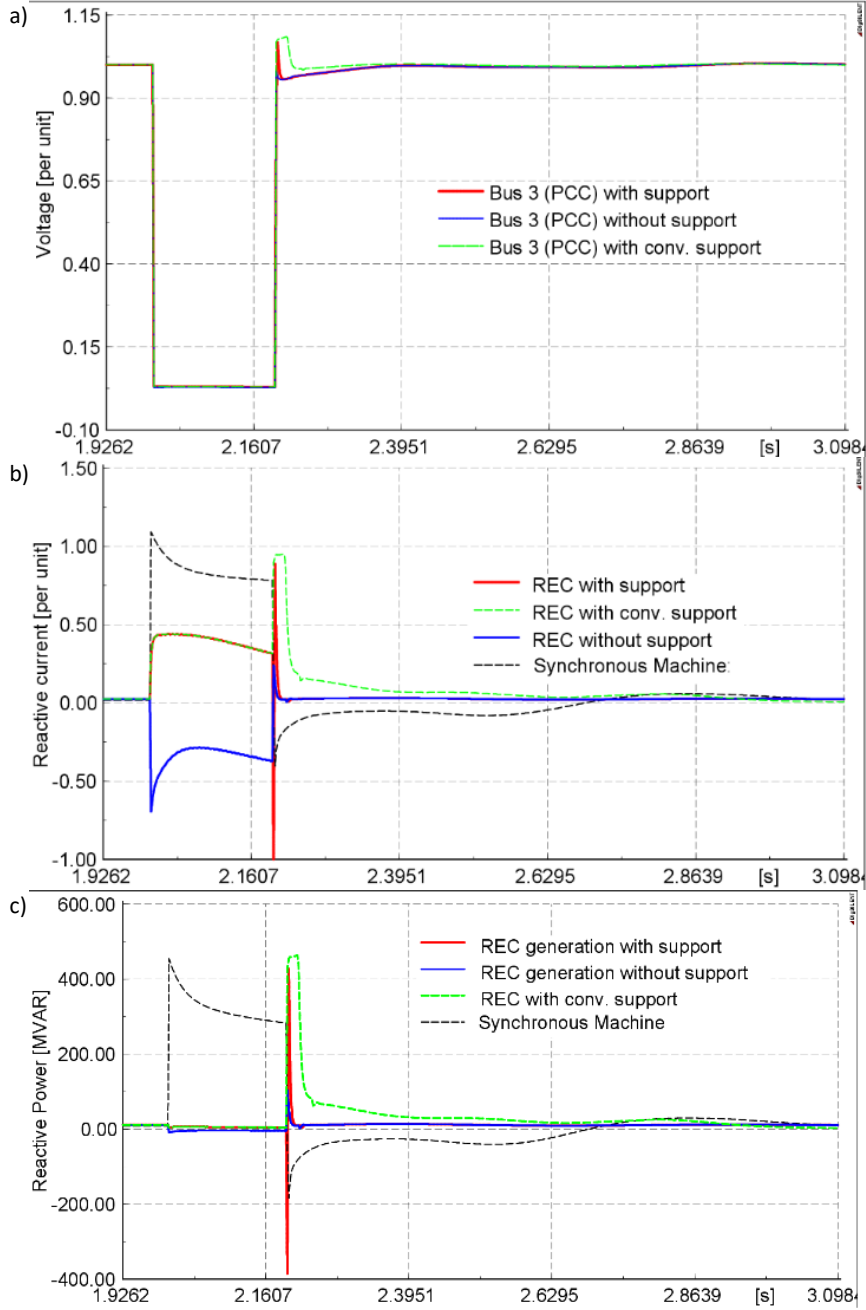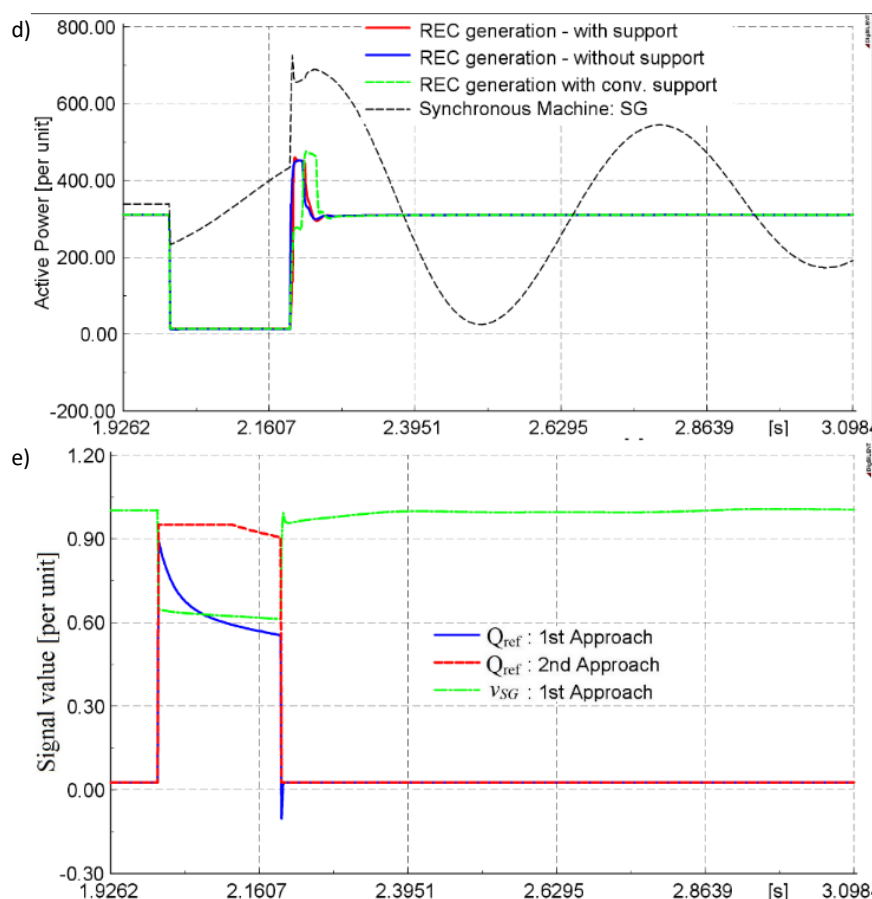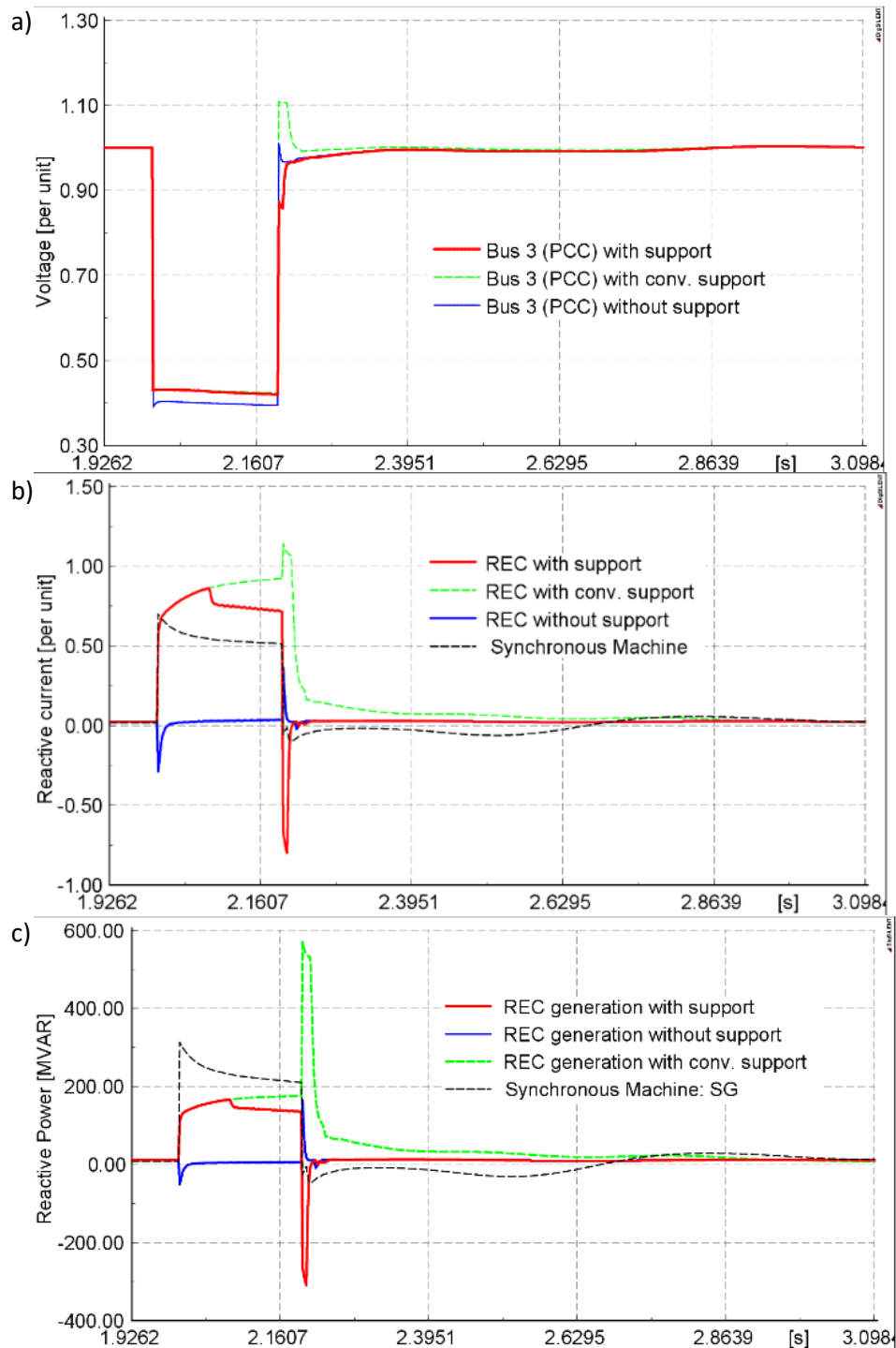
Figure 6. Scenario 1/1st Approach: a) Voltage at PCC, b) Reactive currents, c) Reactive power, d) Active power, and e) Key control signals.

Scenario 2 provides further in-depth analysis for the proposed RAS voltage support due to the alleviated fault severity which provides the opportunity to better observe the performance of support methods. The higher fault impedance mitigated the voltage dip to around 0.46 pu as shown in Figure 7(a), where the impact of support methods can be identified and the voltage dip is improved by about 4%. The reactive compensation capability is clearer in Scenario 2, where the reactive current is almost providing the pattern of the SG but in larger pu value due to the lower voltage at the AC bus of REC compared to v_{SG}. Reactive power aligns with the response of both the REC reactive current and Q_{SG}, however, it does not reach the same magnitude of Q_{SG} due to the different available apparent power of REC and the lower voltage level at REC bus compared to v_{SG}. In addition, a clear difference is observed between conventional support and RAS method, where RAS has the merit of closer response to the SG and recovers faster to unity power factor as soon as the fault is cleared. The RAS method also avoids the reactive power surge caused by the conventional method at the instant of fault clearance, where the RAS method reduces reactive power strongly following the SG. The active power is slightly changed when the RAS controller is applied due to the lower voltage dip in Scenario 2 as shown in Figure 7(d). The RAS method shows an important advantage over the conventional method at the instant of fault clearance where the active power does not severely drop or oscillate. The active power provided by REC is reduced as a natural response to compensate the increase of the required reactive power, i.e. to maintain the apparent power limit of REC, according to the applied RAS voltage support.

The key control signals are shown in Figure 7(e), where the time axis is zoomed-in compared to the other sub-figures to achieve better visualization of the dynamics of the control signals. The voltage at SG is relatively better where it is higher compared to Scenario 1. Similar to Scenario 1, Q_{ref} in 2nd Approach is always higher than Q_{ref} in 1st Approach, however, and Q_{ref} does not reach the reactive power limit, as the fault in Scenario 2 is moderate which leads to less Q_{SG} and higher v_{SG}. Q_{ref} of both approaches has the same pattern, i.e. constant of proportionality is V^o_{PCC}/v_{SG} under this moderate fault.
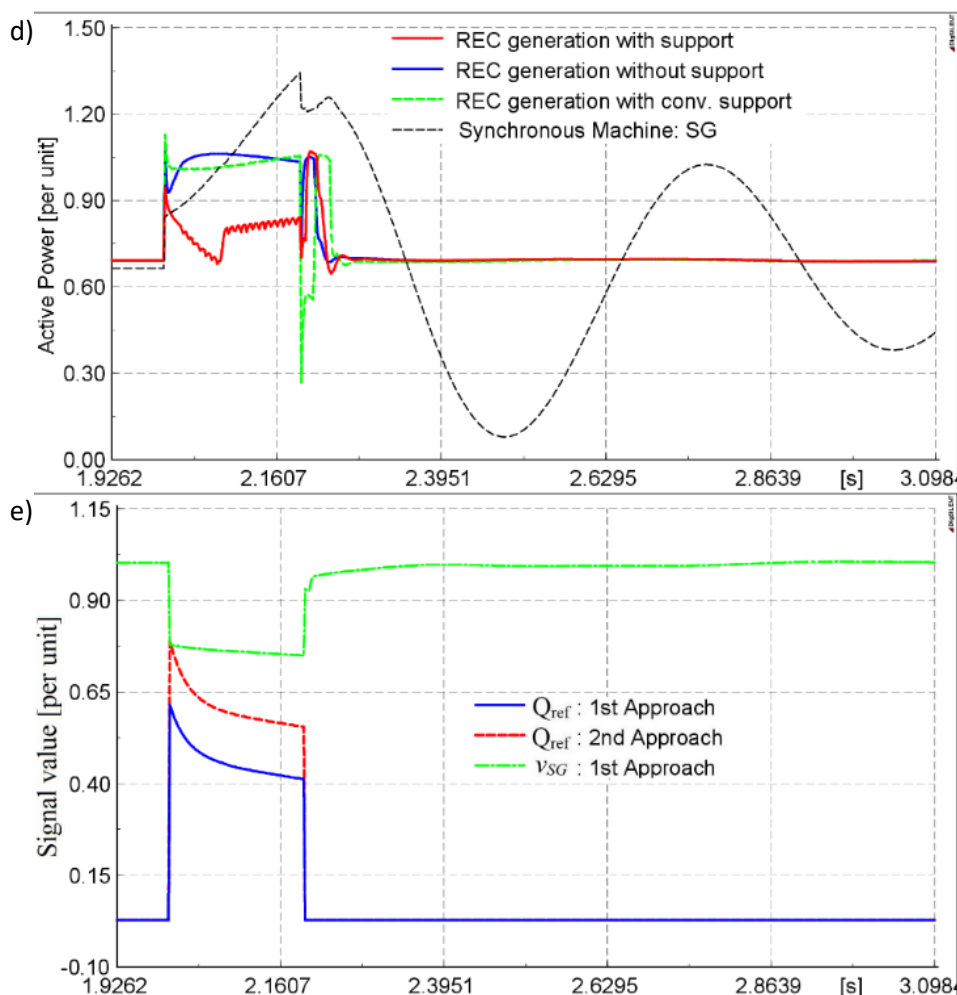
Figure 7. Scenario 2/1st Approach: a) Voltage levels, b) Reactive current, c) Reactive power, d) Active power, and e) Key control signals.

The 2nd Approach under Scenario 2, has a marginal difference compared to 1st Approach in the voltage at the faulted bus as shown in Figure 8(a). However, the provided reactive current is higher at the 2nd Approach, and has an opposite gradient compared to the leader SG as shown in Figure 8(b). The reactive power has a smoother pattern in 2nd Approach compared to 1st Approach, as it relies on Q_{SG} only as shown in Figure 8(c). The active power is marginally changed compared to 1st Approach as shown in Figure 8(d).

In summary, both approaches enable reactive compensation mimicking the profile of reactive power generation of the leader SG. It is worth mentioning that the active power dynamics of both approaches are almost overlaying, hence the active power dynamics are not included in the set of graphs in Figure 8. The deviation between the two approaches is marginal at serious faults, while at moderate dips, the 2nd Approach commonly pushes Q_{ref} to the limit. There is no clear advantage for one of the approaches over each other, however, the 1st Approach can provide a smoother response at moderate dips, while the 2nd Approach requires communicating v_{SG} measurements in addition to the assessment of Q_{SG}.

Further scenarios were executed, for example a fault of very low impedance is applied at the WF internally at the busbar of Ring 2 in Figure 5(b), i.e. collection feeder of 20 WTGs. The integration of RAS voltage support did not have an impact on system transients, due to the occurrence of the fault

offshore, in addition the voltage at Bus 3-SEC was slightly affected. The graphic illustrations of this scenario are not included to avoid over-lengthening the paper.
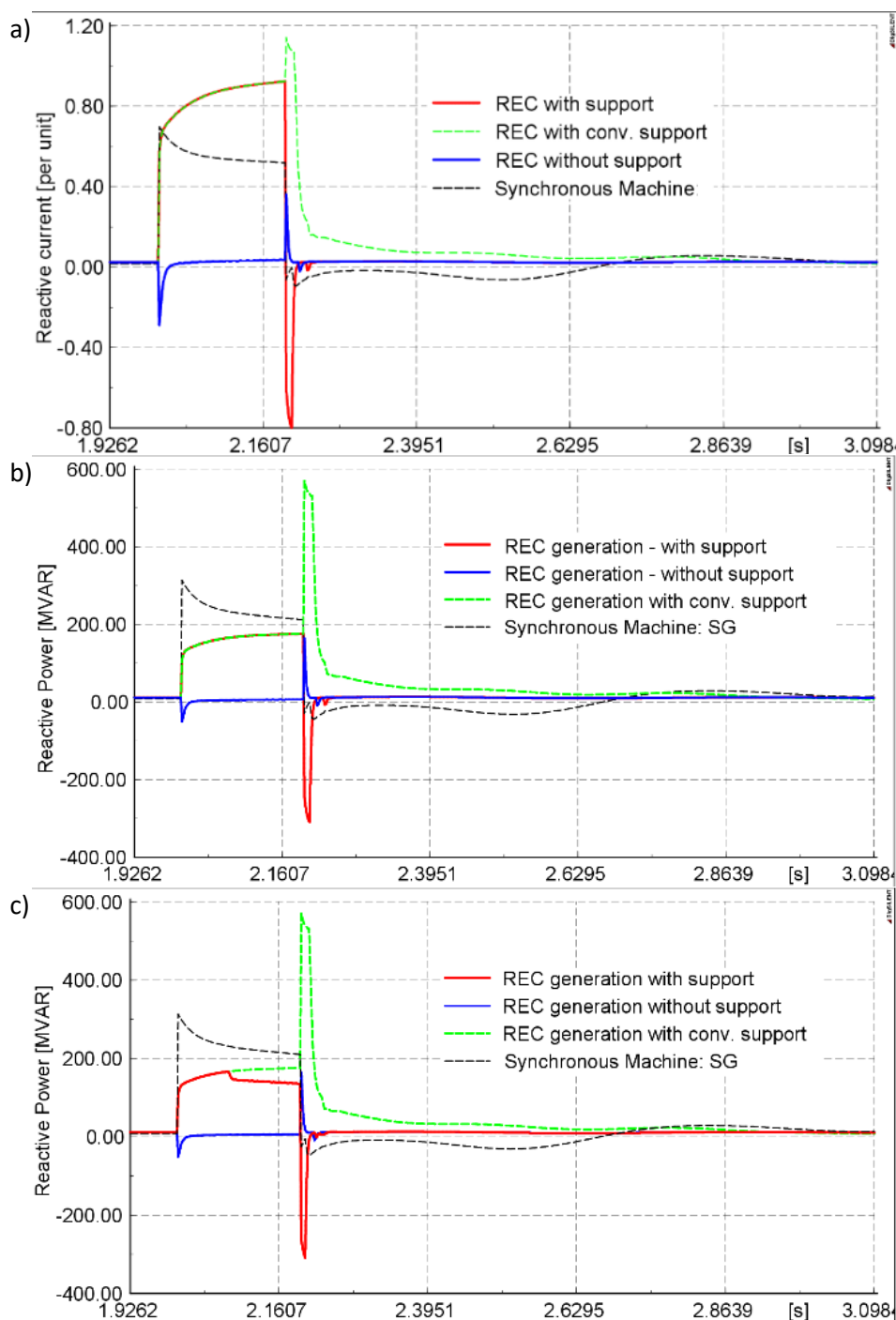

Figure 8. Scenario 2/2nd Approach: a) Voltage levels, b) Reactive current, c) Reactive power

6.2 Frequency events and results

A frequency excursion is enforced by a sudden load change of 100 MW at t = 2s, which initiates a generation-demand imbalance. At t = 4.5s, the SG re-dispatches its output to cover the gap between generation and demand. This scenario is repeated under three cases, without frequency support, with the conventional support method, and with the RAS-based method. When no frequency support is provided by the WF, the WTGs are not de-loaded and produce around 320 MW, which corresponds to a situation of an above-average wind speed. It is of note that, the impact of setting

the de-loading ratio and frequency deadband on the provided support with frequency-based supplementary controllers was investigated by the authors in [33].

The impact of RAS support is clear on the improvement of frequency nadir, however the RoCoF during the very early stage of the event is almost identical for the three case studies as shown in Figure 9(a). The conventional method achieved an almost identical response in case of no-support, except the marginal improvement in the frequency nadir, as the occurring event stimulates higher power support, mainly relying on the setting of f^m_d, i.e. higher f^m_d can neutralize this slight advantage. This case study opted to apply reasonable average wind speed not a very high optimistic profile to examine the proposed method under a normal situation. The frequency nadir has improved with support by about 30 mHz, which is a reasonable improvement taking into consideration the wind power output conditions during the event according to the literature [34]. The frequency also recovers to the safe margin quicker compared to the case without support. The new steady state frequency with and without support is the same for all cases, which is expected as the WF recovers to its initial output, where the provided power support decays gradually after T_{ss} in case of RAS-based method. After the SG is re-dispatched and by the end of T_{ss}, the frequency stabilized at an improved level in case of RAS method. However, the WTG recovers to its normal operation as soon as the frequency is above f_{low} in case of conventional de-loading. The provision of support has almost no impact on the frequency stability of the offshore AC network of the WF, which is reflected by the frequency response at Bus 2 whose graph is not shown to improve figure visibility.

The output active power of the REC and SG are displayed in Figure 9(b) to show the high alignment between both responses. The 20% de-loading is evident through the difference between the red and blue curves. During the early stage of the event, the WF output and SG have the same pattern where the WTGs are associated with the leader SG response as explained earlier. At the end of the sustainability confirmation duration (T_{ss}), the de-loading of WF output recovers gradually, while the SG compensates the gap between generation and demand. Meanwhile, in case of conventional de-loading, the output recovers to the de-loaded margin when the frequency enters the deadband. The voltage levels at both ends of the HVDC link are not affected by the application of the frequency support methods as shown in Figure 9(c).

The key signals of the RAS frequency support are depicted in Figure 9(d), where $\dot{P}_{SG}$ reaches 3 pu/s at the early stage of the event (for the sake of figure clarity, the axis is clipped at 2 pu/s). The application of de-loading is reflected by the ratio between P_{ref} and P^o_{ref}, which is obtained using (1) and (2) according to the applied support method. The droop power support, ΔP_{SG} is kept constant during T_{ss} to ensure that the SG has been dispatched to a new loading level that is adequate to cover the new load demand. Afterwards, de-loading is applied gradually through a certain predetermined rate to avoid any sudden generation-demand imbalance, which can trigger a new frequency event.

It is observed that the role of inertia component ($k_1 \cdot \dot{P}_{SG}/P^m_{SG}$) is temporary relying on the behaviour

of $\dot{P}_{SG}$, which achieves its largest value at the early stage of the frequency event, and then diminishes rapidly. Therefore, it is better to maintain $k_1 < k_2$ to utilise the available reserve, i.e. de-loading margin, in a more efficient way. The key parameters k_1, k_2 and D_F can be tuned to ensure compliance with the enforced grid code. These parameters k_1, k_2 are also tuned to focus the

provided support on either emulated inertia ($k_1 > k_2$) or buying the system more time to re-dispatch conventional generation assets ($k_1 < k_2$).
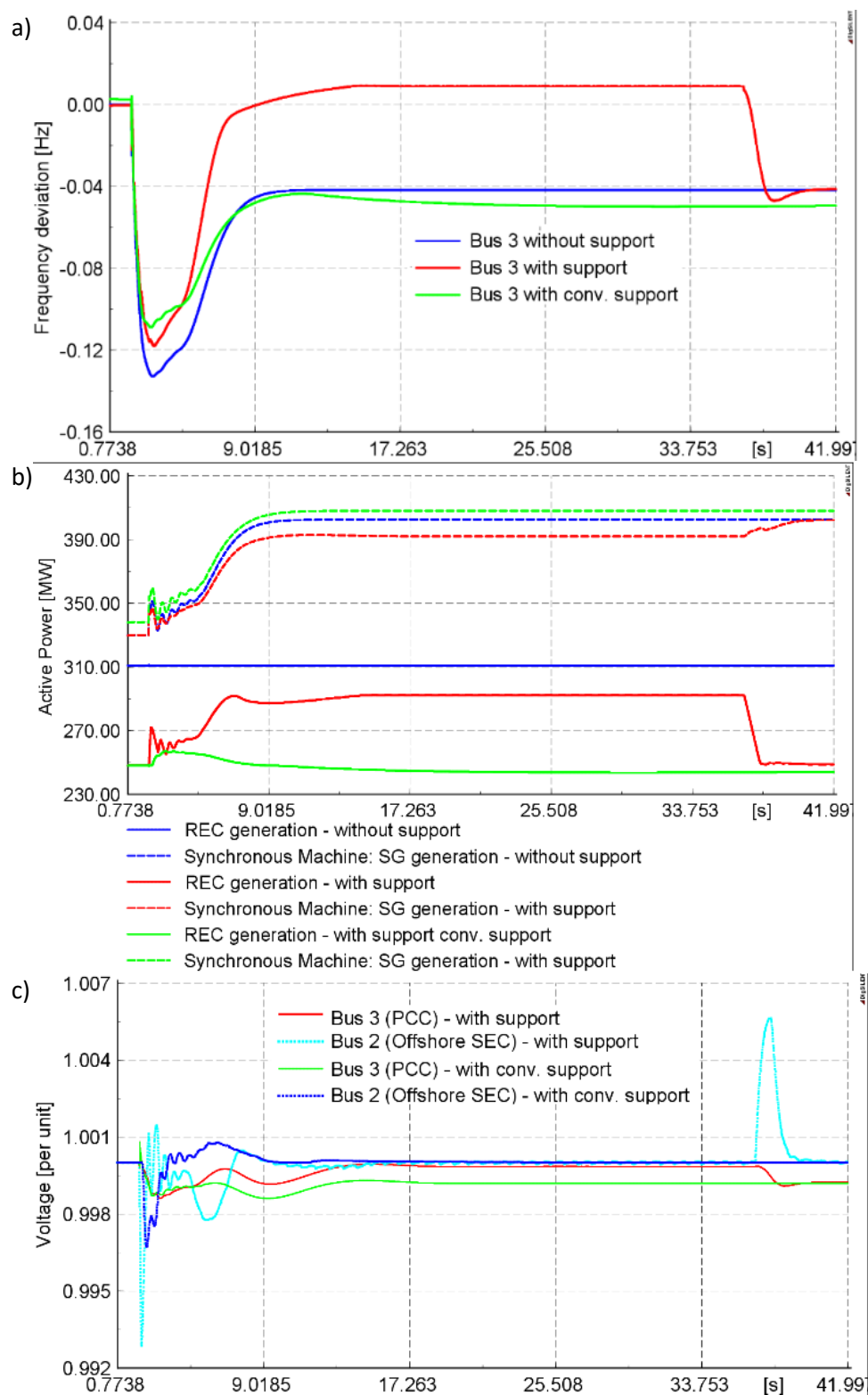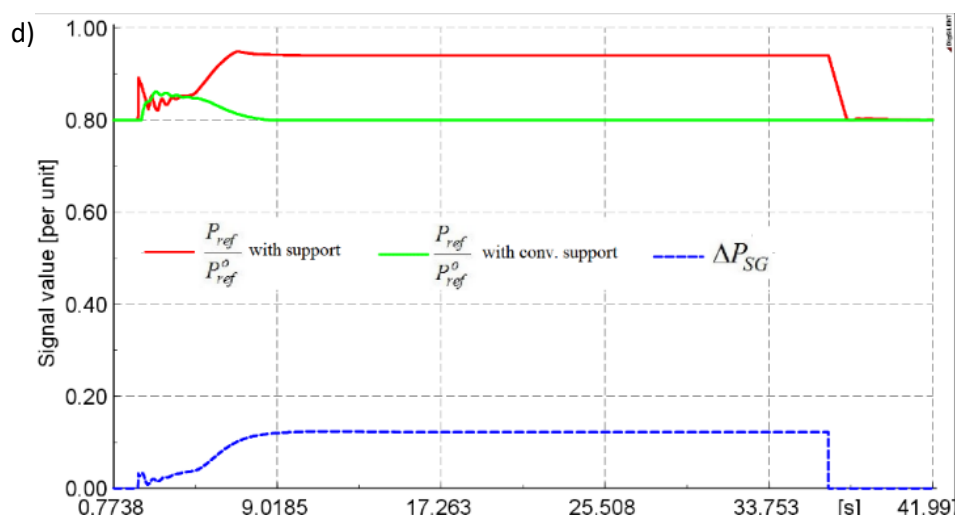
Figure 9. Frequency support implementation; a) Frequency response; b) Active power generation;
c) Voltage response; and d) Relevant control signals of the applied support method

5. Conclusions

This paper presents a novel concept to coordinate between the power electronics-interfaced renewable energy systems and conventional synchronous generators. The frequency and voltage support are provided by an offshore wind farm, relying on this novel concept and compared to conventional voltage and frequency support methods. The paper applies this to a single offshore wind farm that follows a certain generator. However, expanding the concept application to more wind farms, where each follows a different SG across the grid should be applicable, because each farm responds as an additional generating unit of the conventional power plant that is associated with, during severe events only.

The obtained results reflect the benefits, feasibility and ease of application of such concept. The main merits are avoiding frequency measurements, mitigate the volume of communicating data to the wind turbines, wind farms and converter stations, and the proximity of the obtained response to that of a synchronous power plant. It also allows earlier event detection and facilitate the compliance with grid codes. The proposed control methods to utilize this novel concept are not the only applicable methods, where further methods can be developed to copy the response of a synchronous power station by an onshore or offshore wind power plant or any other renewable energy systems. However, the proposed voltage and frequency support methods proved to be reliable and have a positive impact on system dynamics through the applied case studies using a commercial simulation software. The synchronous generator location can have an impact in case of voltage support as the synchronous generator sees different voltage dip compared to the one seen at the connection point of the renewable energy system which is also investigated and treated by the second approach of voltage support. Meanwhile, the deviations between the frequency responses at different locations across are minor, and hence the location of the leader synchronous generator does not have a major influence on the provision of frequency support using this concept.

Appendix

Table 3. Key parameters of WTG model (DFIG)

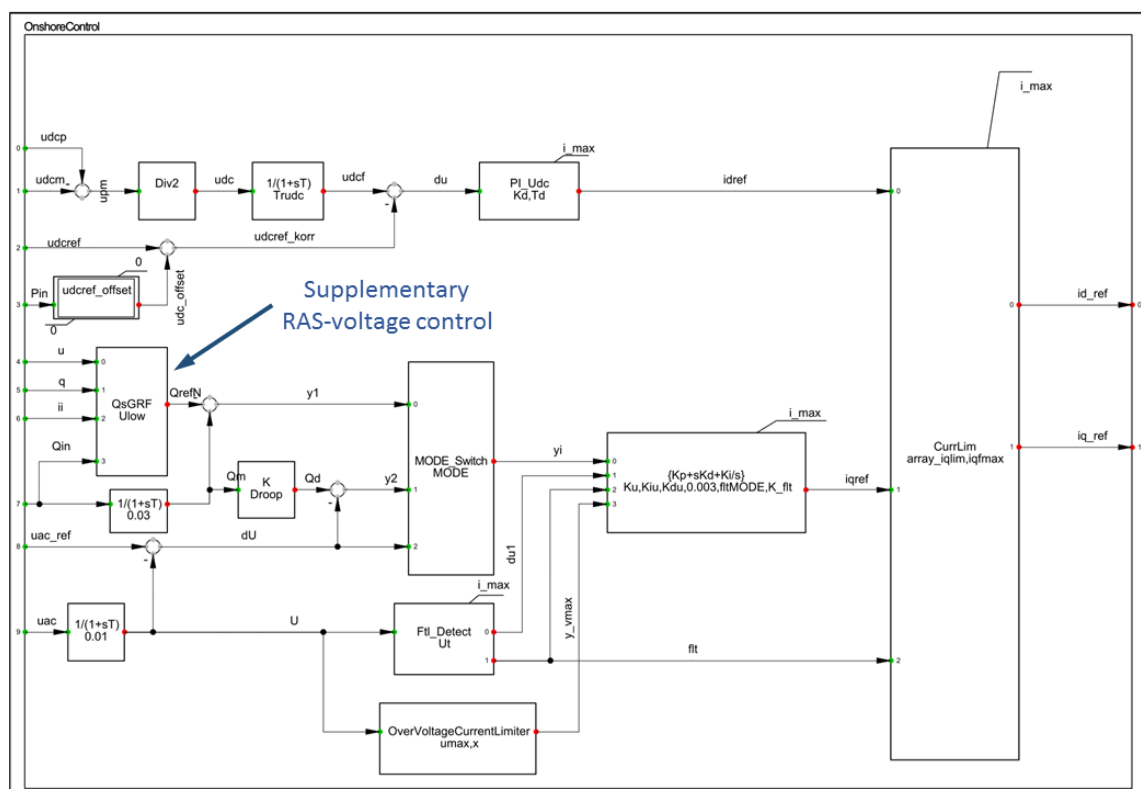| Turbine and drive train		Converter and control	
Rated power	5 MW	P & Q control time constants	0.1s
Terminal voltage	0.69 kV	P & Q control gains	4
Inertia	4s	Speed control PI gains	1, 0.1
Shaft damping factor	1.5	Combined current limit	1.3 pu

Figure 10. The supplementary RAS voltage support control as integrated to the generic DIgSILENT WTG library model

Table 4. Key parameters of SG model

Voltage regulator and exciter		Turbine and governor	
Measurement delay	20ms	Inertia	4s
Controller gain	200	Turbine factor	0.8
Controller time constant	50ms	Governor time constant	0.4s
Exciter constant	1	Servo time constant	0.6s
Exciter time constant	0.5s	Valve opening rate	0.3 s^{-1}

Table 5. Key parameters of the REC model

Circuit elements and control			
Capacitance to ground	200 μF	Current limit	1.05
Series reactor impedance	0.15 pu	Reactive power limits	± 0.95 pu
PLL PI gains	30, 3	Gain of DC voltage control	10
AC voltage PI control (K_I)	100	Time constant of DC voltage control	0.1s
AC voltage PI control (K_P)	12	Reactive current limit	1 pu

References

[1] European Network of Transmission System Operators for Electricity (ENTSO-e), "Research, innovation and development roadmap 2017-2026,", 2017, Available: riroadmap.entsoe.eu/wp-content/uploads/2016/.../entsoe_ri_roadmap_2017-2026.pdf

[2] European Commision, "Communication from the Commission to the European Parliament, the Council, the European Economic and Social Committee and the Committee of the Regions, Energy Roadmap," Belgium, 2012, Available: ec.europa.eu/energy/sites/ener/files/documents/2012_energy_roadmap_2050_en_0.pdf.

[3] T. Burton, D. Sharpe, N. Jenkins, and E. Bossanyi, Wind energy handbook, John Wiley & Sons Ltd, 2001.

[4] P. Kundur, Power System Stability and Control. New York: McGraw-Hill Inc., 1994.

[5] J. Lee, E. Muljadi, P. Sorensen, and Y. C. Kang, "Releasable Kinetic Energy-Based Inertial Control of a DFIG Wind Power Plant," IEEE Transactions on Sustainable Energy, vol. 7, no. 1, pp. 279-288, 2016.

[6] A. B. Attya and T. Hartkopf, "Wind turbine contribution in frequency drop mitigation - modified operation and estimating released supportive energy," IET Generation Transmission & Distribution, vol. 8, no. 5, pp. 862-872, 2014.

[7] L.-R. Chang-Chien and Y.-C. Yin, "Strategies for Operating Wind Power in a Similar Manner of Conventional Power Plant," IEEE Transactions on Energy Conversion, vol. 24, no. 4, pp. 926-934, 2009.

[8] N. R. Ullah, T. Thiringer, and D. Karlsson, "Temporary primary frequency control support by variable speed wind turbines - Potential and applications," IEEE Transactions on Power Systems, vol. 23, no. 2, pp. 601-612, 2008.

[9] I. D. Margaris, S. A. Papathanassiou, N. D. Hatziargyriou, A. D. Hansen, and P. Sorensen, "Frequency Control in Autonomous Power Systems With High Wind Power Penetration," IEEE Transactions on Sustainable Energy, vol. 3, no. 2, pp. 189-199, 2012.

[10] S. Wang, J. Hu, X. Yuan, and L. Sun, "On Inertial Dynamics of Virtual-Synchronous-Controlled DFIG-Based Wind Turbines," IEEE Transactions on Energy Conversion, vol. 30, no. 4, pp. 1691-1702, 2015.

[11] Y. Hirase, K. Abe, K. Sugimoto, K. Sakimoto, H. Bevrani, and T. Ise, "A novel control approach for virtual synchronous generators to suppress frequency and voltage fluctuations in microgrids," Applied Energy, vol. 210, pp. 699-710, 2018.

[12] A. Malik and J. Ravishankar, "A hybrid control approach for regulating frequency through demand response," Applied Energy, vol. 210, pp. 1347-1362, 2018.

[13] M. Rezkalla, A. Zecchino, S. Martinenas, A. M. Prostejovsky, and M. Marinelli, "Comparison between synthetic inertia and fast frequency containment control based on single phase EVs in a microgrid," Applied Energy, vol. 210, pp. 764-775, 2018.

[14] M. Tsili and S. Papathanassiou, "A review of grid code technical requirements for wind farms," IET Renewable power generation, vol. 3, no. 3, pp. 308-332, 2009.

[15] M. Ezzat, M. Benbouzid, S. Muyeen, and L. Harnefors, "Low-voltage ride-through techniques for DFIG-based wind turbines: state-of-the-art review and future trends," in 39th Annual Conference of the IEEE Industrial Electronics Society, 2013.

[16] T. K. Vrana, L. Trilla, and A. Attya, "Development of a generic future grid code regarding wind power in Europe," presented at the 16th Wind Integration Workshop, 2017. Available: https://strathprints.strath.ac.uk/62533/

[17] J. Vidal, G. Abad, J. Arza, and S. Aurtenechea, "Single-Phase DC Crowbar Topologies for Low Voltage Ride Through Fulfillment of High-Power Doubly Fed Induction Generator-Based Wind Turbines," IEEE Transactions on Energy Conversion, vol. 28, no. 3, pp. 768-781, 2013.

[18] X. Zhang, Z. Wu, M. Hu, X. Li, and G. Lv, "Coordinated Control Strategies of VSC-HVDC-Based Wind Power Systems for Low Voltage Ride Through," Energies, vol. 8, no. 7, pp. 7224-7242, 2015.

[19] J. A. Suul, A. Luna, P. Rodríguez, and T. Undeland, "Virtual-Flux-Based Voltage-Sensor-Less Power Control for Unbalanced Grid Conditions," IEEE Transactions on Power Electronics, vol. 27, no. 9, pp. 4071-4087, 2012.

[20] L. Yang, Z. Xu, J. Ostergaard, Z. Y. Dong, and K. P. Wong, "Advanced Control Strategy of DFIG Wind Turbines for Power System Fault Ride Through," IEEE Transactions on Power Systems, vol. 27, no. 2, pp. 713-722, 2012.

[21] A. B. Attya and O. Anaya-Lara, "Provision of frequency support by offshore wind farms connected via HVDC links," in 5th IET International Conference on Renewable Power Generation, London, 2016.

[22] J. Ma, Y. Qiu, Y. Li, W. Zhang, Z. Song, and J. S. Thorp, "Research on the Impact of DFIG Virtual Inertia Control on Power System Small-Signal Stability Considering the Phase-Locked Loop," IEEE Transactions on Power Systems, vol. 32, no. 3, pp. 2094-2105, 2017.

[23] Y. Tan, L. Meegahapola, and K. M. Muttaqi, "A Suboptimal Power-Point-Tracking-Based Primary Frequency Response Strategy for DFIGs in Hybrid Remote Area Power Supply Systems," IEEE Transactions on Energy Conversion, vol. 31, no. 1, 2016.

[24] F. D. Bianchi, J. L. Domínguez-García, and O. Gomis-Bellmunt, "Control of multi-terminal HVDC networks towards wind power integration: A review," Renewable and Sustainable Energy Reviews, vol. 55, pp. 1055-1068, 3// 2016.

[25] J. R. Arribas, A. F. Rodríguez, Á. H. Muñoz, and C. V. Nicolás, "Low voltage ride-through in DFIG wind generators by controlling the rotor current without crowbars," Energies, vol. 7, no. 2, pp. 498-519, 2014.

[26] K. NARENDRA and T. WEEKES, "Phasor Measurement Unit (PMU) communication experience in a utility environment," presented at the Conference on Power Systems, 2008.

[27] S. S. Yu, T. K. Chau, T. Fernando, and H. H. C. Iu, "An Enhanced Adaptive Phasor Power Oscillation Damping Approach With Latency Compensation for Modern Power Systems," IEEE Transactions on Power Systems, vol. 33, no. 4, pp. 4285-4296, 2018.

[28] DIgSILENT GmbH, "DIgSILENT Technical Documentation: HVDC Connected Offshore Wind Farm," ed. Gomaringen, Germany: DIgSILENT GmbH, 2015.

[29] DIgSILENT GmbH, "Dynamic Modeling of Doubly-Fed Induction Machine Wind-Generators," ed. Gomaringen, Germany: DIgSILENT GmbH, 2008.

[30] C. Li-Jun and I. Erlich, "Doubly Fed Induction Generator Controller Design for the Stable Operation in Weak Grids," Sustainable Energy, IEEE Transactions on, vol. 6, no. 3, pp. 1078-1084, 2015.

[31] NEPLAN, "Turbine-Governor models," Switzerland2012, Available: https://www.neplan.ch/wp-content/uploads/2015/08/Nep_TURBINES_GOV.pdf.

[32] NEPLAN, "Exciter models," Switzerland2012, Available: https://www.neplan.ch/wp-content/uploads/2015/08/Nep_EXCITERS1.pdf.

[33] A. B. Attya, O. Anaya-Lara, and W. E. Leithead, "Novel metrics to quantify the impacts of frequency support provision methods by wind power," in 2016 IEEE PES Innovative Smart Grid Technologies Conference Europe (ISGT-Europe), Ljubljana, 2016.

[34] A. B. Attya, J. L. Dominguez-Garcia, and O. Anaya-Lara, "A review on frequency support provision by wind power plants: Current and future challenges," Renewable and Sustainable Energy Reviews, vol. 81, pp. 2071-2087, 2018.